

ity, can result in the FCHL phenotype. Although decreased LDL receptor activity is not thought to be the primary defect in human FCHL (1, 2), LDL cholesterol and APOB amounts appear to be influenced by LDL receptor activity (21). In APOC3 transgenic mice, hypertriglyceridemia arises from a delay in clearance of VLDL (7), reflecting an *in vivo* lipolysis defect (7, 22), which may be caused by decreased binding of VLDL to endothelial cell proteoglycans, impairing access to LPL (22–24). It is possible that low LDL receptor activity results in increased conversion of accumulating VLDL into IDL and LDL. Other hypertriglyceridemia genes also might produce the FCHL phenotype. For example, deficiency of LPL activity has been found in some FCHL families (6, 25). Although this is not usually because of alterations in the LPL gene itself (25), other genes that diminish LPL activity might underlie FCHL in some instances.

REFERENCES AND NOTES

1. J. L. Goldstein, H. G. Schrott, W. R. Hazzard, E. L. Bierman, A. G. Motulsky, *J. Clin. Invest.* **52**, 1544 (1973).
2. J. D. Brunzell *et al.*, *J. Lipid Res.* **24**, 147 (1983).
3. P. Cullen, B. Farren, J. Scott, M. Farrall, *Arterioscler. Thromb.* **14**, 1233 (1994).
4. A. P. Wojciechowski *et al.*, *Nature* **349**, 161 (1991). The genes for apolipoproteins A-I, C-III, and A-IV form a cluster on chromosome 11 [G. A. Bruns, S. K. Karathanasis, J. L. Breslow, *Arteriosclerosis* **4**, 97 (1984)]. These genes encode apoproteins involved in the formation and metabolism of VLDL and HDL.
5. C.-F. Xu *et al.*, *Clin. Genet.* **46**, 385 (1994).
6. S. P. Babirak *et al.*, *Arterioscler. Thromb.* **12**, 1176 (1992).
7. Y. Ito, N. Azrolan, A. O'Connell, A. Walsh, J. L. Breslow, *Science* **249**, 790 (1990); K. Aalto-Setälä *et al.*, *J. Clin. Invest.* **90**, 1889 (1992).
8. S. Ishibashi *et al.*, *J. Clin. Invest.* **92**, 833 (1994).
9. M. J. Callow, L. J. Stoltzfus, R. M. Lawn, E. M. Rubin, *Proc. Natl. Acad. Sci. U.S.A.* **91**, 2130 (1994); G. Chiesa *et al.*, *J. Clin. Invest.* **32**, 23747 (1993).
10. L. B. Agellon *et al.*, *J. Biol. Chem.* **266**, 10796 (1991); X.-C. Jiang, L. B. Agellon, A. Walsh, J. L. Breslow, A. R. Tall, *J. Clin. Invest.* **90**, 1290 (1992).
11. Analysis of the plasma lipoprotein triglyceride distribution by gel filtration chromatography showed an increase in IDL-LDL triglyceride (858 mg/dl) and HDL triglyceride (57 mg/dl) in LDLR0/C3/CETP mice compared with IDL-LDL triglyceride (350 mg/dl) and HDL triglyceride (10 mg/dl) in LDLR0/C3 mice.
12. J. M. Dietschy, S. D. Turley, D. K. Spady, *J. Lipid Res.* **34**, 1637 (1993).
13. S. Venkatesan, P. Cullen, P. Pacy, D. Halliday, J. Scott, *Arterioscler. Thromb.* **13**, 1110 (1993); J. D. Brunzell, A. D. Sniderman, J. J. Albers, P. O. Kwiterovich Jr., *Arteriosclerosis* **4**, 79 (1984).
14. T. Hayek *et al.*, *J. Clin. Invest.* **96**, 2071 (1995).
15. C. J. Fielding and P. E. Fielding, *J. Lipid Res.* **36**, 211 (1995).
16. M. Dammerman, L. A. Sandkuij, J. L. Halaas, W. Chung, J. L. Breslow, *Proc. Natl. Acad. Sci. U.S.A.* **90**, 4562 (1993); Q. Zeng *et al.*, *Hum. Genet.* **95**, 371 (1994).
17. M. R. Hayden *et al.*, *Am. J. Hum. Genet.* **40**, 421 (1987).
18. G. M. Dallinga-Thie *et al.*, *J. Lipid Res.* **37**, 136 (1996).
19. W. W. Li *et al.*, *J. Clin. Invest.* **96**, 2601 (1995).
20. B. Staels *et al.*, *ibid.* **95**, 705 (1995); S. Haubenwallner *et al.*, *J. Lipid Res.* **36**, 2541 (1995).
21. S. M. Grundy, A. Chait, J. D. Brunzell, *Arteriosclerosis* **7**, 203 (1987).
22. K. Aalto-Setälä *et al.*, *J. Lipid Res.* **37**, 1802 (1996).
23. Z.-S. Ji, S. Fazio, Y.-L. Lee, R. W. Mahley, *J. Biol. Chem.* **269**, 2764 (1994).
24. N. S. Schacter *et al.*, *J. Clin. Invest.* **98**, 846 (1996).
25. W.-S. Yang, D. N. Nevin, R. Peng, J. D. Brunzell, S. S. Deeb, *Proc. Natl. Acad. Sci. U.S.A.* **92**, 4462 (1995); E. Gagne, J. Genest Jr., H. Zhang, L. A. Clarke, M. R. Hayden, *Arterioscler. Thromb.* **14**, 1250 (1994).
26. K. A. Kieft, T. M. A. Bocan, B. R. Krause, *J. Lipid Res.* **32**, 859 (1991). Diluted samples of pooled plasma from groups of five or six mice were analyzed by using Superose 6 HR column chromatography to fractionate the lipoproteins. Total cholesterol and triglyceride concentrations were determined by enzymatic assay on total plasma or lipoprotein fractions. Separated lipoproteins in the column eluant were quantified by an online column enzymatic assay for cholesterol or by enzymatic assay of individual fractions. All cholesterol profiles are normalized to represent a constant amount of plasma injected.
27. E. M. Rubin, R. M. Krauss, E. A. Spangler, J. G. Verstuyft, S. M. Clift, *Nature* **353**, 265 (1991).
28. We thank L. Royer for help in quantifying APOA1 in α -HDL and pre- β -HDL. APOB transgenic mice were provided by E. R. Rubin. Supported by NIH grants HL 54591 and HL 21006.

11 September 1996; accepted 18 November 1996

Linkage of G Protein-Coupled Receptors to the MAPK Signaling Pathway Through PI 3-Kinase γ

Marco Lopez-Illasaca,* Piero Crespo,* P. Giuseppe Pellici, J. Silvio Gutkind,† Reinhard Wetzker

The tyrosine kinase class of receptors induces mitogen-activated protein kinase (MAPK) activation through the sequential interaction of the signaling proteins Grb2, Sos, Ras, Raf, and MEK. Receptors coupled to heterotrimeric guanine triphosphate-binding protein (G protein) stimulate MAPK through $G_{\beta\gamma}$ subunits, but the subsequent intervening molecules are still poorly defined. Overexpression of phosphoinositide 3-kinase γ (PI3K γ) in COS-7 cells activated MAPK in a $G_{\beta\gamma}$ -dependent fashion, and expression of a catalytically inactive mutant of PI3K γ abolished the stimulation of MAPK by $G_{\beta\gamma}$ or in response to stimulation of muscarinic (m2) G protein-coupled receptors. Signaling from PI3K γ to MAPK appears to require a tyrosine kinase, Shc, Grb2, Sos, Ras, and Raf. These findings indicate that PI3K γ mediates $G_{\beta\gamma}$ -dependent regulation of the MAPK signaling pathway.

The muscarinic receptor m2 was expressed in COS-7 cells together with an epitope-tagged MAPK (HA-ERK2) (1). Treatment of cells with the agonist carbachol induced activation of MAPK, and wortmannin, an inhibitor of phosphoinositide 3-kinases (PI3Ks), nearly abolished this effect (Fig. 1A). Furthermore, MAPK activation induced by transient expression of $G_{\beta\gamma}$ or by coexpression of $G_{\beta\gamma}$ and the guanine nucleotide exchange factor Sos was also inhibited by wortmannin (Fig. 1B). In contrast, no effect of wortmannin was observed when MAPK was stimulated by epidermal growth factor (EGF); by a mutationally activated form of MEK, MEK E; or by a membrane-targeted form of Sos, myrSos (Fig. 1, A and

B). These results support an essential role for wortmannin-sensitive PI3K in signal transduction from G protein-coupled receptors to MAPK (2), separately from the EGF signaling pathway and upstream of Sos and MEK.

Several species of PI3K have been cloned and characterized. Heterodimeric PI3K α and PI3K β , consisting of p110 catalytic subunits and different p85 adapter molecules, are regulated by receptors with intrinsic or associated tyrosine kinase activity (3). Another PI3K isotype, termed PI3K γ , can be activated *in vitro* by both α and $\beta\gamma$ subunits of heterotrimeric G proteins but does not interact with p85 (4). We expressed the α and γ forms of PI3K in COS-7 cells and investigated their ability to induce MAPK activity (Fig. 2, A and B). PI3K γ induced a concentration-dependent stimulation of MAPK. In contrast, expression of PI3K α or a mutant of PI3K γ lacking lipid kinase activity, PI3K γ K799R (5), did not affect MAPK activity (Fig. 2, B and C). Stimulation of MAPK by overexpression of PI3K γ (5) was abolished by wortmannin (Fig. 2C). These observations indicate that PI3K γ may mediate the wortmannin-sensitive activation of MAPK by receptors linked to heterotrimeric G proteins.

We found that expression of the mutated PI3K γ that lacks lipid kinase activity

M. Lopez-Illasaca and R. Wetzker, Max Planck Research Unit Molecular Cell Biology, Medical Faculty, University of Jena, 07747 Jena, Germany.

P. Crespo and J. S. Gutkind, Molecular Signaling Unit, Oral and Pharyngeal Cancer Branch, National Institute of Dental Research, Bethesda, MD 20892, USA.

P. G. Pellici, Istituto di Medicina Interna e Scienze Oncologiche, Laboratorio di Biologia Molecolare, Policlinico Monteluce, University of Perugia and European Institute of Oncology, Via Ripamonti 435, 20141 Milan, Italy.

* These authors contributed equally to this work.

† To whom correspondence should be addressed at the Molecular Signaling Unit, Oral and Pharyngeal Cancer Branch, National Institute of Dental Research, National Institutes of Health, 9000 Rockville Pike, Building 30, Room 212, Bethesda, MD 20892-4330, USA.

nearly abolished MAPK activation induced by expression of m2 receptors and by stimulation with carbachol, or by expression of $G_{\beta\gamma}$ (Fig. 2D). However, no inhibitory effect by this mutant was observed when MAPK was stimulated with EGF or in $G_{\beta\gamma}$ -induced activation of phospholipase C- β_2 (PLC- β_2) (Fig. 2E). Thus, the mutated PI3K γ appears to specifically inhibit the MAPK response to $G_{\beta\gamma}$. We also expressed a chimeric molecule combining the extracellular and transmembrane domain of CD8 fused to the COOH-terminal domain of β ARK, which includes the $\beta\gamma$ -binding region (6). This chimeric molecule expressing the CD8 antigen at the cell surface and the β ARK COOH-terminal domain at the inner face of the plasma membrane is expected to bind and sequester free $\beta\gamma$, thus blocking $\beta\gamma$ -dependent pathways (6). As expected, CD8- β ARK inhibited activation of PLC- β_2 by $G_{\beta\gamma}$ (Fig. 2E). Coexpression of CD8- β ARK with PI3K γ nearly abolished MAPK activation by PI3K γ , whereas CD8 alone had no demonstrable effect (Fig. 2F). CD8- β ARK was ineffective

in inhibiting MAPK activation by PI3K γ when this kinase was expressed as a myristoylated form, upon fusing its coding region to that of the NH₂-terminal myristoylation, membrane localization signal from c-Src (7). These results indicate that one function of $G_{\beta\gamma}$ is to localize PI3K γ to the plasma membrane, thereby allowing access to lipid substrates. We can conclude that PI3K γ has a critical role linking G protein-coupled receptors and $G_{\beta\gamma}$ to the MAPK signaling pathway.

We tested whether the small guanosine triphosphate (GTP)-binding protein Ras participates in signal transduction from PI3K γ to the MAPK cascade. The dominant negative mutant N17-Ras suppressed the increase of MAPK activity induced by PI3K γ , but the negative mutants of the small guanosine

triphosphatases (GTPases) RhoA, Rac, and Cdc42 did not (Fig. 3, A and B). Expression of a dominant negative mutant of Raf or a mutant Sos protein lacking the domain involved in Ras-specific guanine nucleotide exchange activity, Sos Δ cdc25, also inhibited MAPK stimulation by PI3K γ without affecting MAPK elevation by the activated form of MEK, MEK E (Fig. 3, C and D). These results support a crucial role for Ras, Raf, and Sos in signaling from G protein-dependent receptors, $G_{\beta\gamma}$, and PI3K γ to the MAPK pathway.

Finally, we investigated the possible involvement of Shc and Grb2 in this signaling route. These elements of the receptor tyrosine kinase-stimulated signaling cascade participate in $G_{\beta\gamma}$ -dependent signal transduction (8). Wortmannin inhibited binding of Shc

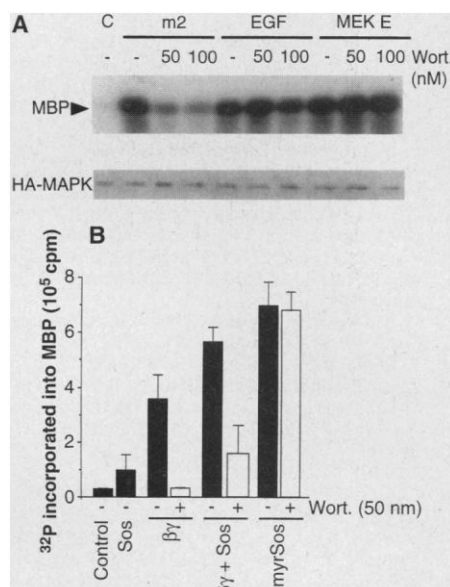
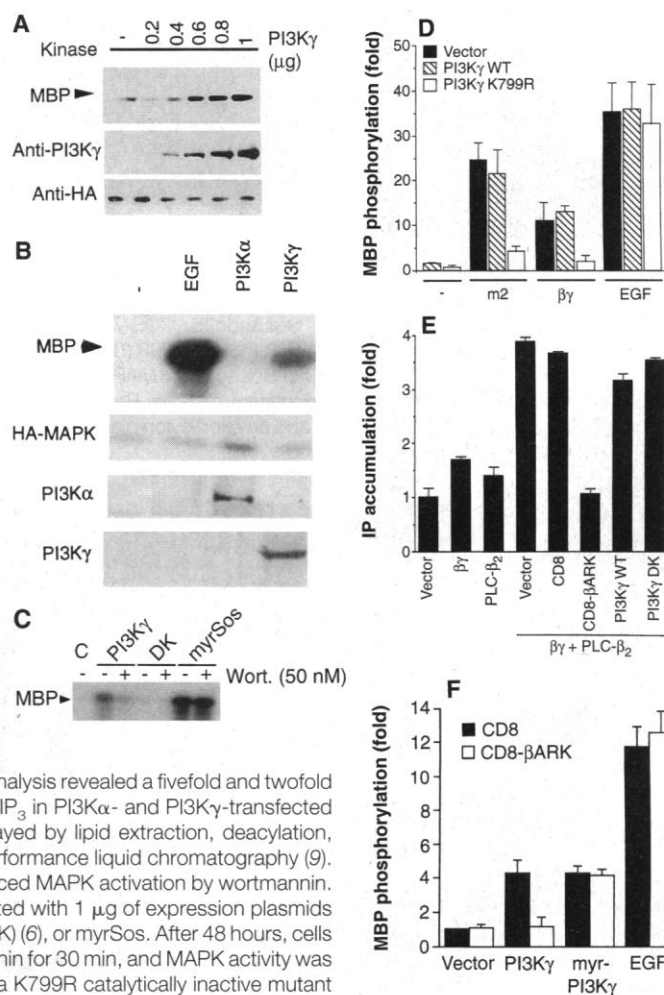


Fig. 1. Inhibition of MAPK activation in COS-7 cells by wortmannin (Wort.). (A) Effect of wortmannin on the stimulation of MAPK induced by the m2 muscarinic receptor and carbachol (m2), EGF, or MEK E. C, control. Two days after transfection (18) with expression plasmids of HA-MAPK and, as indicated, the m2 receptor or MEK E, cells were treated for 5 min with 1 mM carbachol or EGF (100 ng/ml) and the indicated concentration of wortmannin, which was added 20 min before agonist addition. MAPK activity was assayed in cellular lysates (19). (B) Wortmannin blocked MAPK activation induced by $G_{\beta\gamma}$. COS-7 cells transfected with expression plasmids for the G-protein subunits (G_{β_1} and G_{γ_2}), alone or together with Sos, or cells transfected with myrSos alone were treated with wortmannin, and MAPK activity was assayed.

Fig. 2. MAPK activation by PI3K γ in COS-7 cells. (A) Stimulation of MAPK activity by overexpression of PI3K γ . COS-7 cells were transfected with the indicated amounts of the expression plasmid pEF-BOS PI3K γ . After 2 days, cells were lysed, MAPK activity was assayed (19), and protein immunoblot analysis with antiserum to PI3K γ or with antibody to HA (for the HA-tagged MAPK) was performed (20). (B) Overexpression of PI3K γ but not PI3K α enhances MAPK activity. COS-7 cells were transfected with 1 μ g of expression plasmids for PI3K γ or PI3K α . After 2 days, cells were lysed, MAPK activity was assayed (19), and protein immunoblot analysis with antiserum to PI3K γ and PI3K α was performed. Phospholipid analysis revealed a fivefold and twofold increase in total levels of PIP₃ in PI3K α - and PI3K γ -transfected cells, respectively, as assayed by lipid extraction, deacylation, and separation by high-performance liquid chromatography (9). (C) Inhibition of PI3K γ induced MAPK activation by wortmannin. COS-7 cells were transfected with 1 μ g of expression plasmids for PI3K γ , PI3K γ K799R (DK) (6), or myrSos. After 48 hours, cells were treated with wortmannin for 30 min, and MAPK activity was determined. (D) Effects of a K799R catalytically inactive mutant of PI3K γ on MAPK activation induced by carbachol through m2 receptors, $G_{\beta\gamma}$, or EGF. Empty vector or expression plasmids for PI3K γ wild type (WT), the PI3K γ K799R mutant (6), and the m2 receptor or $G_{\beta\gamma}$ were used for transfection. MAPK activity was assayed after 48 hours. (E) Effects of the K799R catalytically inactive mutant of PI3K γ on phosphatidylinositol hydrolysis induced by $G_{\beta\gamma}$. IP, inositol phosphates. Empty vector or expression plasmids for PI3K γ WT, the PI3K γ K799R mutant (DK), $G_{\beta\gamma}$, PLC- β_2 , CD8, or CD8- β ARK were used for transfection. Forty-eight hours later, the accumulation of [³H]IP for 30 min after addition of LiCl was determined (21). (F) Requirement for interaction of PI3K γ with $G_{\beta\gamma}$ and its possible role in membrane localization. COS-7 cells were cotransfected with different constructs of PI3K γ in the presence or absence of CD8 or the CD8- β ARK expression plasmid, and the effect on MAPK activity was assayed.

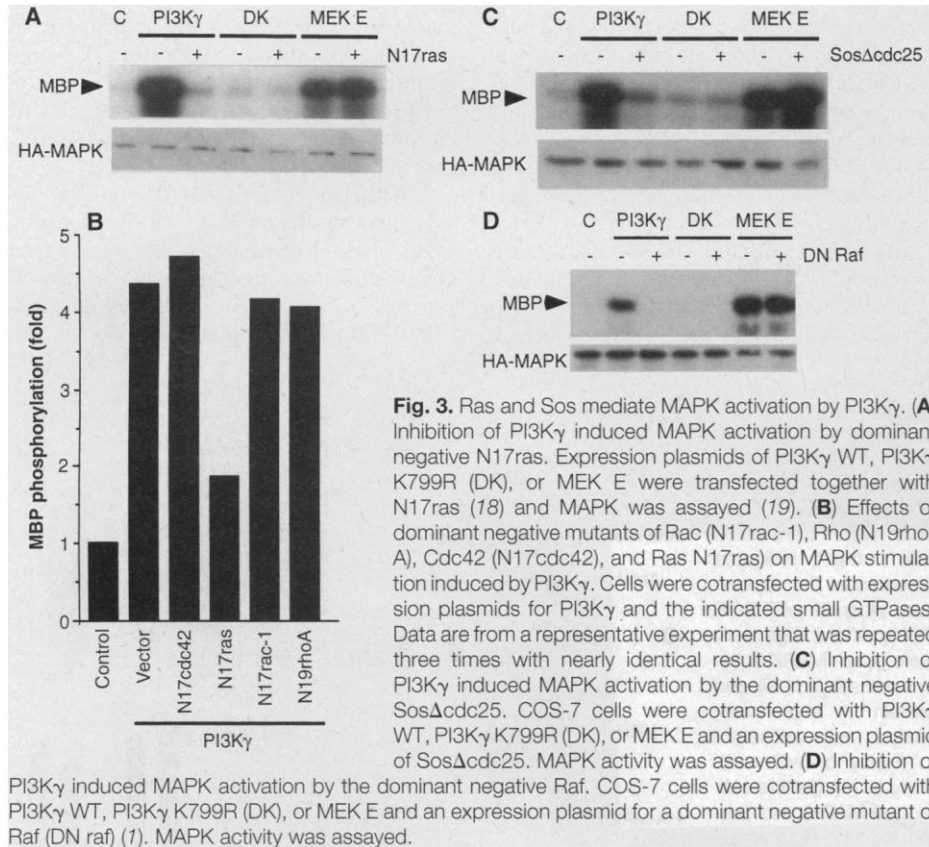


and Grb2 induced by carbachol (Fig. 4A). Association of Shc with Grb2 was induced by expression of PI3K γ in COS-7 cells (9). Expression of PI3K γ also stimulated tyrosine-phosphorylation of Shc (Fig. 4B). Further-

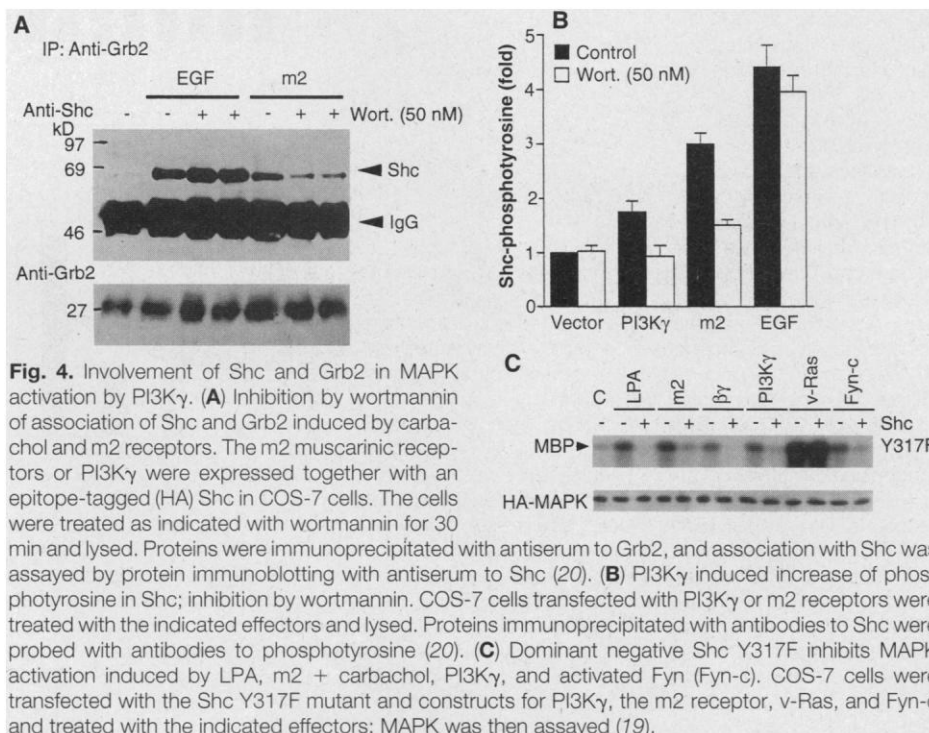
more, a mutant of Shc lacking the tyrosine-phosphorylation site, Y317F (10), suppressed the stimulation of MAPK induced by phosphatidic acid (LPA), expression of G $\beta\gamma$, carbachol in m2-transfected cells, expression

of PI3K γ , or expression of the Src-related tyrosine kinase Fyn (11) (Fig. 4C). In contrast, the Shc mutant did not affect MAPK activation induced by coexpression of v-Ras. Thus, stimulation of MAPK by PI3K γ apparently requires a tyrosine kinase that, in turn, phosphorylates Shc and induces its association with Grb2 and leads to a Ras-dependent activation of MAPK. Consistent with this conclusion, the nonspecific tyrosine kinase inhibitor genistein or the Src-like specific inhibitor PP1 (12) potentially blocked MAPK activation by PI3K γ (9).

The emerging picture is that agonist-activated G protein-coupled receptors first cause the exchange of guanosine diphosphate bound to G α for GTP, thereby causing the dissociation of G $\beta\gamma$ from GTP-bound G α . Free G $\beta\gamma$ would then recruit PI3K γ to the plasma membrane, enhancing the activity of a Src-like kinase (13), which in turn leads to the activation of the Shc-Grb2-Sos-Ras pathway, resulting in increased MAPK activity.



PI3K γ induced MAPK activation by the dominant negative Raf. COS-7 cells were cotransfected with PI3K γ WT, PI3K γ K799R (DK), or MEK E and an expression plasmid for a dominant negative mutant of Raf (DN raf) (7). MAPK activity was assayed.



REFERENCES AND NOTES

1. P. Crespo, N. Xu, W. F. Simonds, J. S. Gutkind, *Nature* **369**, 418 (1994).
2. B. E. Hawes, L. M. Luttrell, T. van Biesen, R. J. Lefkowitz, *J. Biol. Chem.* **271**, 12133 (1996); I. Ferby *et al.*, *ibid.*, p. 11684; C. Knall *et al.*, *ibid.*, p. 2799.
3. R. Kapeller and L. C. Cantley, *Bioessays* **16**, 565 (1994).
4. B. Stoyanov *et al.*, *Science* **269**, 690 (1995).
5. The mutant of PI3K γ that lacks lipid kinase activity, PI3K γ K799R (designated DK) exhibits less than 0.1% of the specific activity of the wild-type enzyme when expressed in vitro. It was provided by M. Wymann, Fribourg (14). Lysine 799 is the wortmannin-binding site of PI3K γ (S. Stoyanova *et al.*, in preparation).
6. W. J. Koch, B. E. Hawes, L. F. Allen, R. J. Lefkowitz, *Proc. Natl. Acad. Sci. U.S.A.* **91**, 12706 (1994).
7. T. Takeya and T. Hanafusa, *Cell* **32**, 881 (1983).
8. T. van Biesen *et al.*, *Nature* **376**, 781 (1995).
9. M. Lopez-Illasaca and R. Wetzker, unpublished data.
10. A. E. Salcini *et al.*, *Oncogene* **9**, 2827 (1994).
11. B. Li *et al.*, *Proc. Natl. Acad. Sci. U.S.A.* **93**, 1001 (1996).
12. J. H. Hanke *et al.*, *J. Biol. Chem.* **271**, 695 (1996).
13. Y. Chen *et al.*, *EMBO J.* **15**, 1037 (1996); L. M. Luttrell *et al.*, *J. Biol. Chem.* **271**, 19443 (1996); A. Ptasznik, A. Traynor-Kaplan, G. M. Bokoch, *ibid.* **270**, 19969 (1995); B. Schieffer *et al.*, *ibid.* **271**, 10329 (1996); J. Sadoshima and S. Izumo, *EMBO J.* **15**, 775 (1996); Y. Wan, T. Kurosaki, X.-Y. Huang, *Nature* **380**, 541 (1996).
14. M. Wymann *et al.*, *Mol. Cell. Biol.* **16**, 1722 (1996).
15. Wild-type PI3K γ was cloned into a modified version of the pEF-BOS vector (M. Lopez-Illasaca, P. Crespo, P. G. Pellici, J. S. Gutkind, R. Wetzker, unpublished data). The construct expressed in COS-7 cells caused an increase in phosphatidylinositol-3,4,5-trisphosphate (PIP $_3$) as assayed by lipid extraction, deacylation, and separation by thin-layer chromatography. The myr-PI3K γ was generated by subcloning of the wild-type construct into pcDNA3-myr, a modified pcDNA3 expression plasmid encoding the 21 NH $_2$ -terminal amino acids of chicken c-Src (16). The cDNAs for human RhoA, Rac1 and Cdc42Hs GTP-binding proteins, activated MEK1 (designated MEK E), and myrSos were generated as described (16). CDB and CDB- β ARK1 were generated as described (17).
16. O. A. Coso *et al.*, *Cell* **81**, 1137 (1995).
17. P. Crespo *et al.*, *J. Biol. Chem.* **270**, 25259 (1995).
18. COS-7 cells were cultured in Dulbecco's modified

Eagle's medium supplemented with fetal bovine serum (10%). Subconfluent cells were transfected with pcDNA3-HA-MAPK and additional DNAs (15) by the DEAE-dextran technique. The total amount of plasmid DNA was adjusted to 3 to 4 μg per plate with vector DNA (pcDNA3; Invitrogen) when necessary; 2 days later, transfected COS-7 cells were cultured overnight in serum-free medium. Cells were then left untreated or were stimulated with various agents, washed in cold phosphate-buffered saline (PBS), and lysed at 4°C in a buffer containing 20 mM Hepes (pH 7.5), 10 mM EGTA, 40 mM β -glycerophosphate, 1% NP-40, 2.5 mM MgCl_2 , 1 mM dithiothreitol, 2 mM sodium vanadate, 1 mM phenylmethylsulfonylfluoride, aprotinin (20 $\mu\text{g}/\text{ml}$), and leupeptin (20 $\mu\text{g}/\text{ml}$). The lysate was centrifuged at 14,000g for 20 min at 4°C, and proteins were immunoprecipitated and assayed for kinase activity. Equivalent expression of cDNA constructs was verified with the respective antibodies.

19. For the MAPK assay, after centrifugation, proteins from clarified supernatants were immunoprecipitated with monoclonal antibody (mAb) to hemagglu-

tinin 12CA5 (Babco, Berkeley, CA) for 1 hour at 4°C, and immunocomplexes were recovered with Gamma-bind G (Pharmacia). Bound proteins were washed three times with PBS supplemented with 1% NP-40 and 2 mM sodium vanadate, once with 0.5 M LiCl in 100 mM tris (pH 7.5), and once with kinase reaction buffer [10 mM Mops (pH 7.5), 12.5 mM β -glycerophosphate, 7.5 mM MgCl_2 , 0.5 mM EGTA, 0.5 mM sodium fluoride, and 0.5 mM vanadate]. Reactions were done in 30- μl volumes of kinase reaction buffer containing 1 μCi of [γ - ^{32}P] adenosine triphosphate (ATP) per reaction, 20 μM unlabeled ATP, and myelin basic protein (MBP) (1.5 mg/ml) (Sigma) at 30°C for 30 min. Reactions were terminated by addition of 5 \times Laemmli buffer. Samples were boiled and proteins were separated by SDS-polyacrylamide gel electrophoresis (PAGE) (12% gel). Phosphorylated MBP was visualized by autoradiography and quantified with either a phosphorimager or a liquid scintillation detector. Parallel samples were immunoprecipitated with antibody to HA and processed for protein immunoblot analysis

with a MAPK-specific antiserum.

20. Lysates of total cellular protein or anti-HA immunoprecipitates were analyzed by protein immunoblotting after SDS-PAGE with the corresponding rabbit antiserum or mouse mAb. Immunocomplexes were visualized by enhanced chemiluminescence detection (Amersham) with the use of goat antiserum to rabbit or mouse immunoglobulin G coupled to horseradish peroxidase (Cappel, West Chester, PA). Mouse mAbs to the HA epitope 12CA5 were purchased from Babco. Rabbit polyclonal antisera to c-Src, Shc, and Grb2 were purchased from Santa Cruz Laboratories (Santa Cruz, CA) or Upstate Biotechnology (Lake Placid, NY).
21. S. Zhang, O. A. Coso, R. Collins, J. S. Gutkind, W. F. Simonds, *J. Biol. Chem.* **271**, 20208 (1996).
22. We thank A. Gazit and A. Levitzki for supplying PP1, M.L.I. and R.W. are supported by grants SFB 197 and We 1565/1-2 from the Deutsche Forschungsgemeinschaft.

31 July 1996; accepted 22 November 1996

Uniting Two General Patterns in the Distribution of Species

Ilkka Hanski* and Mats Gyllenberg

Two patterns in the distribution of species have become firmly but independently established in ecology: the species-area curve, which describes how rapidly the number of species increases with area, and the positive relation between species' geographical distribution and average local abundance. There is no generally agreed explanation of either pattern, but for both the two main hypotheses are essentially the same: divergence of species along the ecological specialist-generalist continuum and colonization-extinction dynamics. A model is described that merges the two mechanisms, predicts both patterns, and thereby shows how the two general, but formerly disconnected, patterns are interrelated.

The species-area (SA) curve is one of the few universally accepted generalizations in community ecology (1-3), but ecologists have failed to agree on the mechanisms that produce this pattern (3). According to the habitat heterogeneity hypothesis, large areas have more species than small ones because of their greater range of distinct resources, which facilitates the occurrence of ecological specialists (3). As an alternative, MacArthur and Wilson (2) advanced the dynamic theory of island biogeography, which predicts that species richness increases with area owing to decreasing extinction rate with increasing area.

Another general pattern in the distribution of species has been well documented only during the past 15 years (4, 5): species with wide distributions tend to be locally more abundant than species with narrow distributions. We call this relation the dis-

tribution-abundance (DA) curve. The two most widely recognized explanations of the DA curve are Brown's niche breadth hypothesis and metapopulation dynamics. According to Brown's hypothesis (5), generalist species, or species using ubiquitous resources (6), are both locally common and widely distributed, whereas specialists are constrained to have narrow distribution and tend to be locally uncommon. Metapopulation dynamic models predict that locally common species become widely distributed because of their low extinction rates and high colonization rates (7, 8). High migration rates from existing large populations may additionally "rescue" small populations from extinction, in which case a wide distribution with many large populations tends to enhance average local abundance (7).

Surprisingly, although the two main hypotheses about the SA and DA curves are strikingly similar, the two patterns themselves have been studied without any reference to each other (9). To bring conceptual unity to this area of ecology, we demonstrate that the SA and DA curves are both predicted by the same model, which furthermore merges the two "competing" hy-

potheses, namely, ecological specialization (habitat heterogeneity) and extinction-colonization dynamics.

To construct the model, consider a set of R islands (I_0) populated by a "pool" of Q species. The islands differ in area; we denote by m_A and σ_A^2 the mean and the variance of the logarithm of island areas (base e is used throughout this report). Likewise, the species differ in their abundances per unit area (density), with m_w and σ_w^2 denoting the mean and the variance of the logarithm of species densities (11). By definition, the "carrying capacity" (equilibrium population size) of species i on island j is given by $K_{ij} = w_i A_j$, where w_i is the density of species i and A_j is the area of island j .

Following the standard approach to modeling metapopulation dynamics (7), we model changes in the probability $p_{ij}(t)$ of species i being present on island j at time t , in the absence of interspecific interactions, as

$$\frac{dp_{ij}}{dt} = C_i(t)[1 - p_{ij}] - \mu_{ij}p_{ij} \quad (1)$$

where $C_i(t)$ is the colonization rate of empty islands and μ_{ij} is the extinction rate of extant populations. Empirical studies suggest that μ_{ij} is roughly proportional to $1/K_{ij}$ (12, 13), and we use this approximation below. The appropriate expression for $C_i(t)$ is different for two fundamentally different scenarios. In a mainland-island situation, the presence of species on islands is dependent on colonization from a permanent mainland community, where the density of species i is w_i . In this case, $C_i(t)$ is given by $c w_i$, where the value of parameter c decreases with increasing distance to the mainland. In contrast, in the classical metapopulation there is no external mainland, and the empty islands are colonized from other occupied islands (7, 14). Here it is reasonable to assume that the colonization rate of empty islands is proportional

I. Hanski, Department of Ecology and Systematics, University of Helsinki, Post Office Box 17, FIN-00014 Helsinki, Finland.

M. Gyllenberg, Department of Mathematics, University of Turku, FIN-20014 Turku, Finland.

*To whom correspondence should be addressed. E-mail: ilkka.hanski@helsinki.fi